Molecular Orientation of Poly(ethylene naphthalate)/Poly(ethylene terephthalate) Copolymers Utilizing Polarized Raman Spectra

ARTICLE *in* MACROMOLECULES · FEBRUARY 2002

Impact Factor: 5.8 · DOI: 10.1021/ma011229h

Molecular Orientation of Poly(ethylene naphthalate)/Poly(ethylene terephthalate) Copolymers Utilizing Polarized Raman Spectra

A. Soto and G. A. Voyiatzis*

Foundation for Research & Technology-Hellas, Institute of Chemical Engineering and High-Temperature Chemical Processes and Department of Chemical Engineering, University of Patras, P.O. Box 1414, GR-265 00 Patras, Greece

Received July 16, 2001

ABSTRACT: Polarized laser Raman microscopy was used to estimate the molecular orientation of uniaxially drawn films of mostly random copolymers of poly(ethylene 2,6-naphthalate) (PEN) and poly(ethylene terephthalate) (PET) as a function of the draw ratio. The Raman bands of the symmetric stretching modes of benzene and naphthalene rings at 1616 and 1636 cm^{-1} have been respectively used for PET and PEN segments orientation evaluation. Polarized Raman spectra obtained from PEN/PET films in the whole concentration range indicate that PET segments are better oriented in the copolymers than in the homopolymer attenuating the neck formation of PEN. Moreover, PEN/PET films stretched at temperatures 30 °C higher than the corresponding glass transition temperatures exhibit different degrees of segmental relaxation depending on the dominant, PEN or PET, number-average segment length. These relaxation discrepancies are accompanied by conformational changes of the ethylene moieties. In certain PEN/PET polymer mixtures, at specific window of stretching parameters, PEN segments exhibit comparable and even higher homopolymer molecular orientation. Isotropic and drawn type films were both characterized by DSC, solution ^1H NMR, dynamic mechanical tensile measurements, and FT-Raman spectroscopy.

Introduction

The general concept of the effects of processing on material properties is based on the important feature, which simultaneously involves many properties, of whether the material is isotropic or anisotropic. The molecular orientation induced during the processing of polymers by the preferential alignment of macromolecular chains or segments may have a profound influence on their macroscopic physical properties. Many investigations, employing different experimental techniques,[1] like X-ray diffraction,[2] polarized Raman scattering,[3] fluorescence polarization,[4] polarization modulation near-infrared,[5] and mid-infrared linear dichroism,[6] have been undertaken to characterize the orientation distribution of the macromolecular chains or segments of the chains or crystalline regions in polymers. All techniques attempt to approximate the orientation distribution function, $f(\theta)$, which in the case of uniaxially drawn samples relates the number of entities lying in one direction with the angle they make with respect to the draw direction. This function is usually written in an expanded form as a series whose terms are Legendre polynomials.

Roe[7] had at first formulated the expansion of $f(\theta)$, and Bower[8] developed a method to evaluate molecular orientation through the analysis of the Raman scattering intensity of a drawn material. So far, this method has been applied, at times in slightly modified versions, to polyesters,[9] photonic polymers,[10] and industrial polymers.[11] Raman spectroscopy provides information on both the second ($\langle P_2(\cos\theta)\rangle = [3\langle\cos^2\theta\rangle - 1]/2$, θ being the orientation angle) and the fourth ($\langle P_4(\cos\theta)\rangle = [35\langle\cos^4\theta\rangle - 30\langle\cos^2\theta\rangle + 3]/8$) moments of the orientation distribution function, referred to as P_2 and P_4, respectively.[8,12]

* To whom correspondence should be addressed. E-mail gvog@iceht.forth.gr.

It is obvious that the introduction and study of new polymers and/or polymer mixtures can expand the penetration of stretch polymeric materials into new markets.[13] However, the orientation behavior of polymer mixtures is considered complex enough compared to that of homopolymers, and several interpretations have been proposed to explain that in terms of phase separation,[14] free volume,[15] entanglement density,[16] specific interactions,[17] and chain rigidity.[18]

Recently, considerable attention has been paid to PEN/PET copolymers,[19−24] a polymer system that may allow for example the expansion of stretch blow molded bottles to new packaging markets.

Poly(ethylene terephthalate) (PET) has been widely used as one of the important polymers for fibers, films, and food packaging materials because of its high glass transition temperature, T_g, and high melting temperature, T_m. However, its thermal performance and gas barrier properties are not enough to meet requirements for some particular applications such as hot-fill packaging and soft drink containers. On the other hand, poly(ethylene naphthalate) (PEN) is known to possess a higher glass transition temperature and superior oxygen and carbon dioxide barrier properties. PEN can be a good candidate for hot-fill and high barrier packaging applications, but the high cost of PEN has limited its direct applications as a common packaging material.

The objective of the present work is to gain further understanding of the orientation behavior and the mechanisms of deformation in PEN/PET mostly random copolymers in the whole concentration range utilizing polarized Raman spectroscopy.

Experimental Section

Materials. Polyester resins were commercial grade: PET (intrinsic viscosity = 0.94 dL/g in *o*-chlorophenol) was purchased by Goodfellow (UK), and PEN (intrinsic viscosity = 0.69 dL/g in dichloroacetic acid) was kindly supplied by Hoechst Trevira (D). To minimize hydrolysis, polyesters were dried in a vacuum furnace at 120 °C for 24 h and kept in a desiccator

10.1021/ma011229h CCC: $22.00
Published on Web 02/05/2002

Chart 1. Molecular Structures of PET and PEN Homopolymers

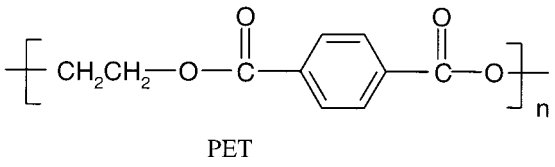

PET

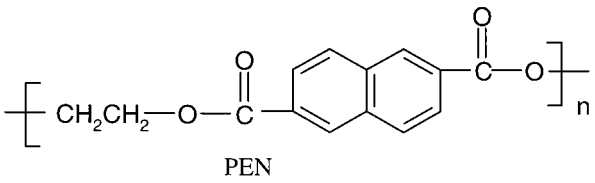

PEN

filled with a "Baker" grade silica gel with indicator. The molecular structures of both homopolymers repeat units are shown in Chart 1.

Sample Preparation. PEN/PET copolymers were prepared by melt mixing under a nitrogen inert atmosphere in a homemade batch mixer at different blending times (10, 20, and 30 min). The polymer mixer consists of a stainless steel vessel (capacity of ~10 g) equipped with a piston (screw speed 12−46 rpm) where working temperature (300 °C) and screw speed (16 rpm) can be easily selected. Uniform polymer films (~200 μm thick) were prepared by melt-pressing the polymer compound between Teflon sheets at 300 °C and 5 MPa followed by quenching in ice water. Clear films were obtained when sufficient transesterification or interchange occurred in the mixer during copolymerization. As a representative example, we mention the PEN/PET (25/75 wt %) films prepared in the batch; after a blending time of only 10 min these films were hazy, presumably due to the low miscibility of PEN and PET, whereas after 30 min clear films were obtained.

Sample Characterization. A TA 2920 differential scanning calorimeter (DSC) operating at a scan rate of 10 °C/min was used to characterize thermal transitions in PEN/PET copolymers. Thermal transitions as well as evaluation of crystallinity levels of each sample were determined from first run DSC scans.

^{1}H NMR Measurements. Solution ^{1}H NMR measurements were performed using a Bruker Avance DPX 400 MHz instrumentation with a magnetic field strength of 9.4 T on specimens prepared by dissolving the master batch in a 1:3 (by volume) mixture of deuterated trifluoroacetic acid and deuterated chloroform in standard NMR tubes (5 mm from Aldrich). The solution concentration was about 2 wt %.

Film Stretching. A dumbbell-shaped test strip with a narrow midsection of 6.5 mm width and 57 mm length films (type II, norm ASTM D 638) were cut from the ~200 μm thick films and stretched in a homemade stretching element constructed according to a modified design previously proposed by Pastor et al.[25] The sample compartment of the stretching element was an isolated glass cylinder where the specimen was attached on a metallic axis bearing two screws spinning, via a motor device, in opposite directions with a strain rate, $\dot{\epsilon}$, that could be easily selected ($\dot{\epsilon} = 0.006-0.2$ s^{-1}). In the sample compartment, the stretching temperature was controlled by a thermocouple, and the heating was accomplished by flushing preheated nitrogen gas. The draw ratio might be preset, and at the moment it was reached, an automatic exchange in the electric valves of nitrogen flow allowed cold nitrogen gas to diffuse into the sample compartment and maintain the orientation already attained. The draw ratio, λ, is the ratio of the extended length to the original length determined from displacement of ink marks on the film strip cut from the narrow midsection of the dumbbell-shaped test strip.

Dynamic Mechanical Measurements. A solid-state analyzer RSA II, Rheometrics Scientific Ltd., was utilized to determine the tensile modulus from isotropic as well as uniaxially drawn polyester films. All dynamic mechanical tensile measurements were performed in the temperature range of 25−40 °C at a frequency of 10 Hz. Specimen dimensions were 2.324 × 0.65 × 0.03 and 2.324 × 0.3 × 0.013 cm^3 for isotropic ($\lambda = 1$) and uniaxially drawn ($\lambda = 4$) polymer films, respectively.

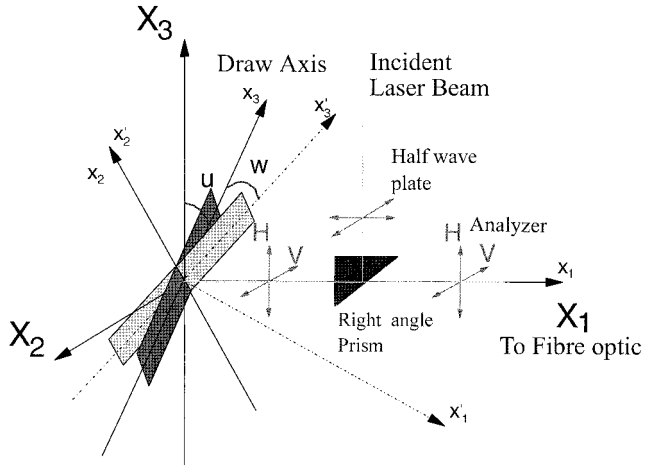

Figure 1. Coordinate axes for backscattering Raman geometry. $OX_1X_2X_3$ are the coordinates axes fixed to the laboratory, and $Ox_1x_2x_3$ are the axes referred to the sample.

Raman Spectroscopy. Fourier transform Raman (FT-Raman) measurements were obtained using a Bruker (D) FRA-106/S component attached to an EQUINOX 55 spectrometer. A R510 diode pumped Nd:YAG polarized laser at 1064 nm (with a maximum output power of 500 mW) was used for Raman excitation in a 180° scattering sample illumination module. An optical filtering reduced the Rayleigh elastic scattering and in combination with a CaF_2 beam splitter and a high-sensitivity liquid N_2-cooled Ge detector allowed the Raman intensities to be recorded from 50 to 3300 cm^{-1} in the Stokes-shifted Raman region, all in one spectrum.

Polarized Raman spectra were mainly recorded using a modified custom-made Dilor Super Head of Jobin Yvon (F)−Horiba (J). The Raman spectra were excited with the linearly polarized light of a solid-state Nd:YAG laser, doubled frequency at 532 nm, attached to the Raman microhead. An ultralong working distance objective (×50) of Olympus (Japan) with pupil adaptation was used for the delivery of the excitation laser beam on the sample. The collected backscattered light was launched onto the core of an optical fiber after being passed through a notch filter. Scattered Raman radiation was dispersed into the spectrograph by a concave grating of 920 grooves/mm and detected by a 1 in. TE-cooled CCD detector. Polarization measurements were performed by using a pair of motorized half-wave plates able to select the polarization direction on the excitation laser beam while a motorized pair of analyzers also permitted the selection of one component on the scattered beam. The spectra were obtained with a power of 15 mW on the specimen for a total integration time of 1 s. This flexible spectroscopic instrumentation, possessing a spectrograph with no moving parts, is able to accumulate integrated fast polarized Raman spectra with a spectral slit width of ~10 cm^{-1}.

The backscattering geometry used in this study is depicted in Figure 1. Two sets of coordinate axes are fixed: one refers to the sample, $Ox_1x_2x_3$, and the second to the experimental setup, $OX_1X_2X_3$. The notation of Raman polarization measurements comprises a combination of three letters, like *h*-VV. The small letter in italics (*h*, *v*, or *d*) denotes the orientation of the draw axis, Ox_3 ($w = 0°$), relative to the laboratory-fixed coordinates, $OX_1X_2X_3$: *h*, when aligned along the OX_3 axis ($u = 0°$); *v*, when aligned along the OX_2 axis ($u = 90°$); and *d*, when aligned at the bisector of the X_3OX_2 angle ($u = 45°$). The two capital letters (HH, HV, VV, or VH) denote the polarization direction of the excitation and scattered light, respectively: H, when the polarization is parallel to the OX_3 axis, and V, when the polarization is parallel to the OX_2 axis.

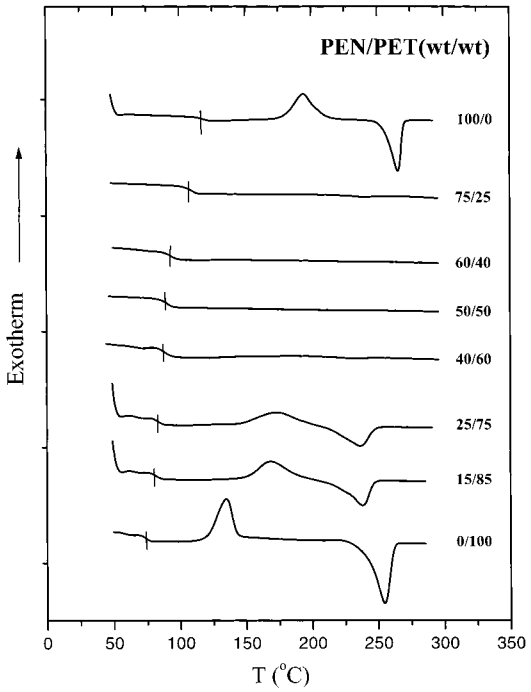

Figure 2. DSC scans first run curves for PEN, PET, and PEN/PET copolymers prepared by melt mixing at 300 °C for 30 min. Short lines indicate the glass transition temperature, T_g.

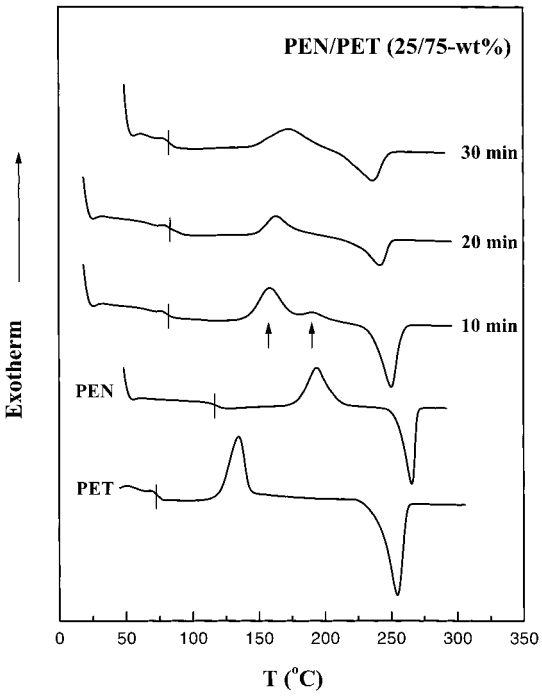

Figure 3. DSC scans first run curves for PEN, PET, and PEN/PET (25/75 wt %) copolymer prepared by melt mixing at 300 °C for three different blending times. Arrows indicate the position of the cold-crystallization exotherms, and short lines point to the glass transition temperatures, T_g's.

Results and Discussion

Polymer Characterization. Figure 2 presents the thermograms of first run DSC scans of PEN and PET homopolymers as well as of PEN/PET copolymers at different compositions. There is evidence of three thermal events in the thermogram: a glass/rubber transition (T_g), a cold crystallization exotherm (T_c), and a melting endotherm (T_m). The glass transition temperature increases monotonically with increasing PEN content from 74 °C in PET to 120 °C in PEN. This observation is consistent with the Fox equation for random copolymers:

$$\frac{1}{T_g} = \frac{w_{PET}}{T_{g,PET}} + \frac{w_{PEN}}{T_{g,PEN}} \quad (1)$$

where w_{PET} and w_{PEN} are the weight fractions of PET and PEN, respectively, in the copolymers.

For PEN/PET (50/50 wt %), there is neither a cold crystallization exotherm nor a melting endotherm; the corresponding sample is amorphous. Copolymers rich in either homopolymer contain measurable levels of crystallinity, as indicated by melting endotherms, which are larger than the cold crystallization exotherms. The weight percent crystallinity was calculated as follows:

$$X_c = \frac{\Delta H_m - \Delta H_c}{\Delta H_f} \times 100 \quad (2)$$

where ΔH_m is the enthalpy of melting determined by DSC, ΔH_c is the absolute value of the enthalpy of cold crystallization determined by DSC, and ΔH_f is the enthalpy of fusion of the crystallites. The enthalpies of fusion for PET and PEN are given as 140 and 103 J/g, respectively.[26] For copolymers, the enthalpy of fusion of the crystallites is taken as that of the homopolymer present in the highest amount. The values of crystallinity obtained are consistent with film preparation. There is no observed crystallinity in samples of intermediate composition, which also supports the concept of mostly random copolymers. The DSC results and weight percent crystallinity in copolymers are resumed in Table 1.

Table 1. Summary of PEN/PET DSC Results

polymer	T_g (°C)	T_c (°C)	T_m (°C)	% X_c
PET	74	134	255	10
PEN/PET (15/85) 30′	81.5	168	238.5	1.6
PEN/PET (25/75) 30′	83.6	172.5	236.5	2.4
PEN/PET (40/60) 30′	88.6		233.9	<1
PEN/PET (50/50) 30′	90.5			
PEN/PET (60/40) 30′	93.7			
PEN/PET (75/25) 30′	109.5		236.5	1
PEN	120	194	265	1

As already reported before,[27] blending time and temperature are the key factors controlling the transesterification in PEN and PET blends. This can be confirmed by the thermograms, shown in Figure 3, from PEN/PET (25/75 wt %) mixtures prepared in the mixer at different reaction times of 10, 20, and 30 min. The PEN/PET (25/75 wt %)−polymer mixture obtained after reaction time of 10 min shows a double cold crystallization exotherm. This indicates that the transesterification is at the first stage and individual polymer segments are still long enough, able to be crystallized. It also appears that the T_g is independent of the blending time (Figure 3), and it exhibits an almost linear dependence on the blend composition (Figure 2), as already invoked elsewere.[21]

To determine the extent of transesterification in the polymer films prepared by melt pressing, solution ^{1}H NMR measurements were performed. For PEN/PET copolymers, the extent of transesterification can be determined by the NMR shift of the ethylenic protons.

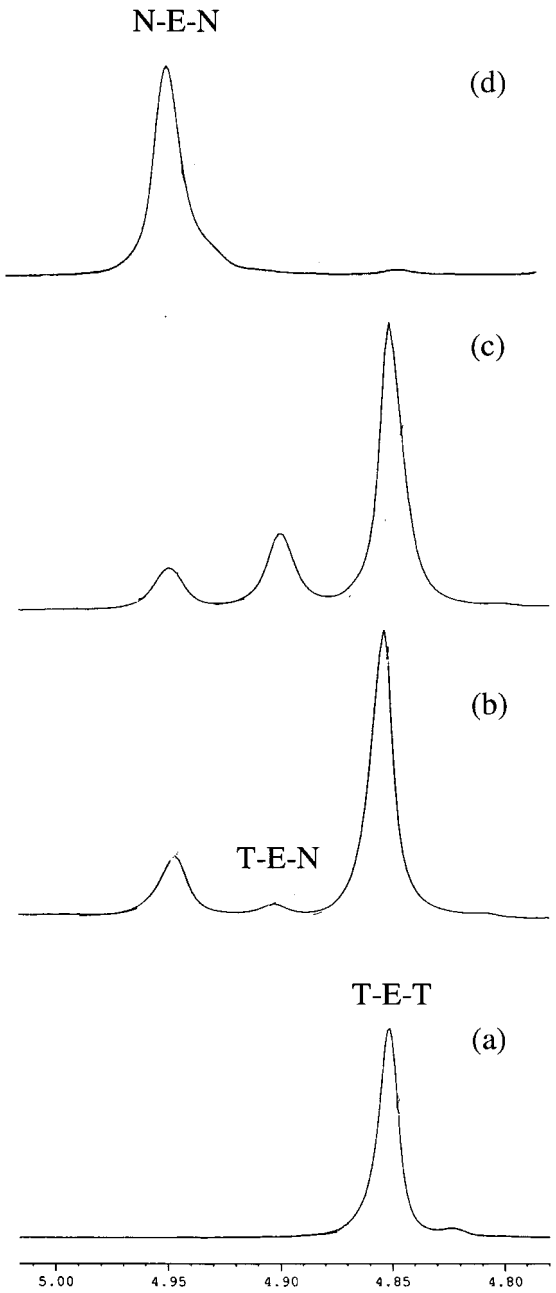

Figure 4. Ethylene peak splitting of ^{1}H NMR spectra for PET (a), PEN/PET (25/75 wt %) copolymers mixed at 300 °C for 10 (b) and 30 min (c), and PEN (d).

This is shown in Figure 4, where the NMR shift of the ethylene link between a terephthalate and a naphthalate group, a T-E-N type link, appears at approximately 4.90 ppm, whereas the corresponding ethylenic links between two terephthalate units, of T-E-T type, and two naphthalate units, of N-E-N type, are located at ~4.85 and 4.95 ppm, respectively. The relative intensity of the peak attributed to T-E-N ethylene links is enhanced with increasing the reaction time, a clear indication of a stepping-up transesterification level. The measure of the integrated intensity of each resonance peak and the use of a statistical data analysis, developed by Yamadera and Murano[28] to investigate the sequence distribution and randomness of copolyesters, gave the opportunity to determine the fraction of transesterification, f_{TEN}, the probability of finding a N (or T) unit next to a T (or N) unit, P_{NT} and P_{TN}, the number-average chain lengths, L_{PET} and L_{PEN}, and the degree of randomness, B ($B = 0$ for block copolymer; $B = 1$ for random copolymer). Results for the whole concentration level are listed in Table 2.

Table 2. NMR Results on the PEN/PET Transesterification Level

	25/75, 10 min[a]	25/75, 20 min	25/75, 30 min	40/60, 30 min	50/50, 30 min	60/40, 30 min	75/25, 30 min
f_{TEN}[b]	0.045	0.086	0.211	0.246	0.267	0.28	0.24
P_{NT}	0.107	0.297	0.464	0.376	0.304	0.255	0.170
P_{TN}	0.028	0.050	0.137	0.183	0.237	0.315	0.403
L_{PEN}	9.34	3.36	2.15	2.66	3.28	3.93	5.87
L_{PET}	35.71	19.73	7.3	5.46	4.205	3.17	2.47
B	0.135	0.347	0.601	0.559	0.54	0.57	0.573

[a] PEN/PET (wt/wt), time of reaction. [b] See text for explanation of symbols.

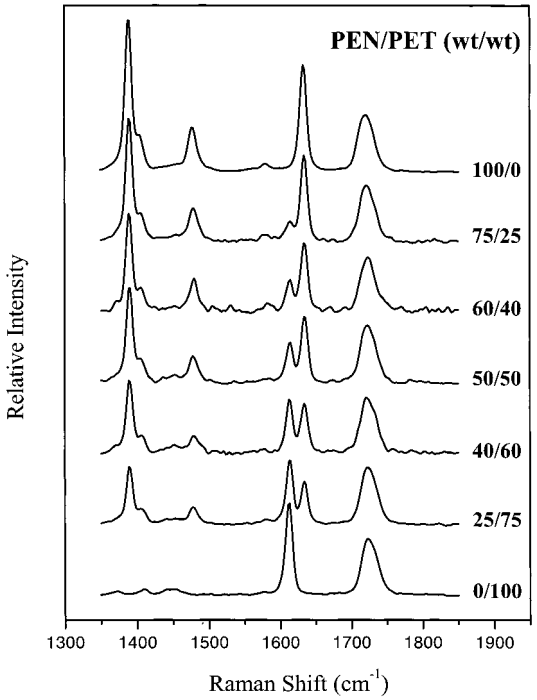

Figure 5. FT-Raman spectra of PEN/PET copolymers in the spectral region of disubstituted phenyl and naphthalene symmetric stretch for the whole concentration range.

Molecular Orientation Studies Using Raman Spectroscopy. Figure 5 shows typical FT-Raman spectra of PEN and PET homopolymers and PEN/PET copolymers in the spectral window of benzene and naphthalene ring stretching modes. The 1636 cm^{-1} peak in PEN is attributed to the 2,6 disubstituted skeletal symmetric vibration of the naphthalene ring, and the 1616 cm^{-1} peak in PET corresponds to the 1,4 para-substituted benzene ring. The Raman peaks in the copolymer correspond to the peaks found for the homopolymers, PEN and PET; there are no new peaks as a result of copolymerization. In the copolymers, the 1636 and 1616 cm^{-1} Raman bands represent corresponding PEN and PET segments. Because of the partial overlapping of these two peaks, their band intensities were measured after curve fitting; this was performed using the PeakFit v4.0 software of Jandel Scientific. Although a mixed Gaussian−Lorentzian function was used, the peaks were found to be predominantly Lorentzian; for both peaks, the area of the Raman bands was used as the intensity value.

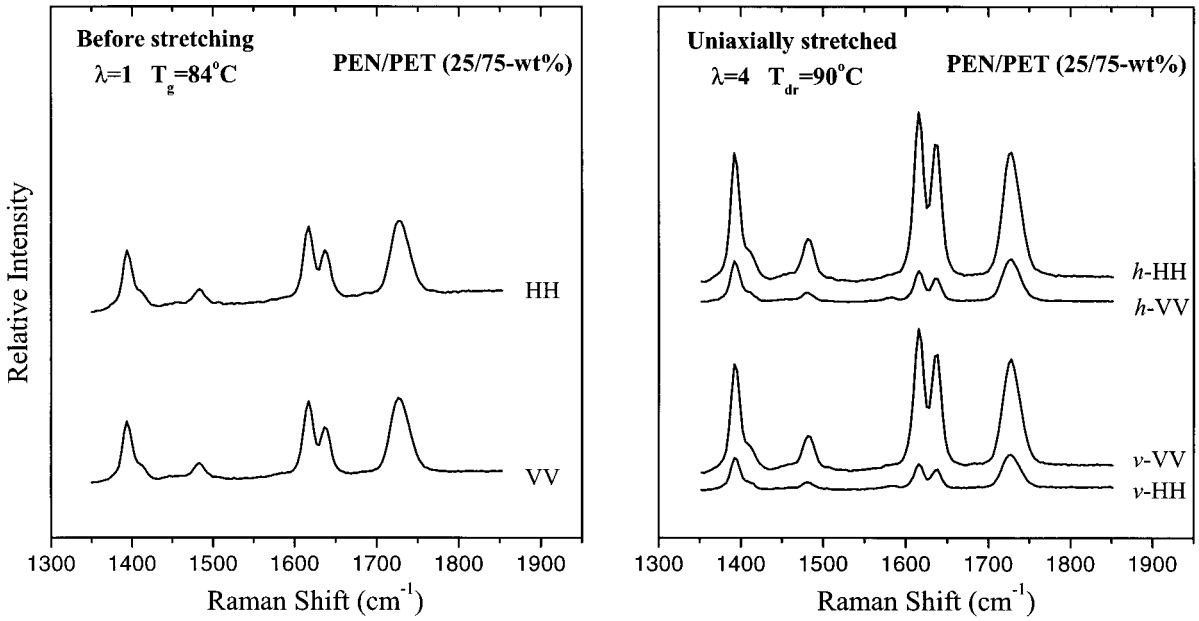

Figure 6. Polarized Raman spectra of PEN/PET (25/75 wt %) films before (on the left) and after (on the right) uniaxial drawing (draw ratio $\lambda = 4$), in two different polarization geometries, VV and HH, with respect to the position of the specimen, *v* or *h*, relative to the laboratory-fixed coordinates. The spectra are shifted along the intensity axis for clarity.

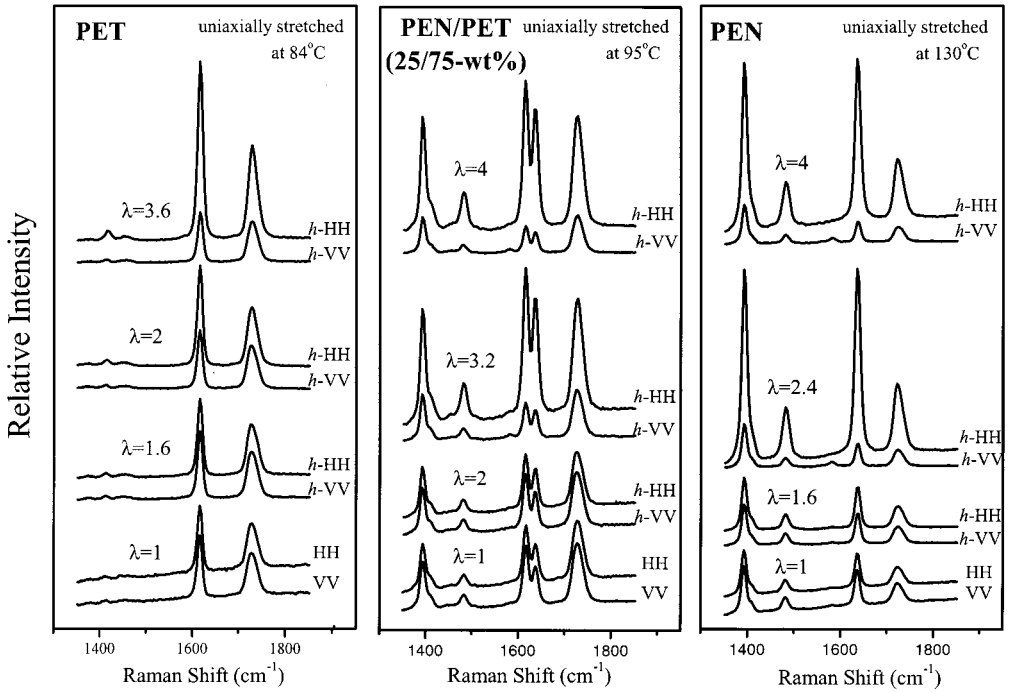

Figure 7. Polarized Raman spectra of PEN (on the right), PET (on the left), and PEN/PET (25/75 wt %) copolymer (in the center) specimens uniaxially stretched at various draw ratios.

In Figure 6, typical polarized Raman spectra are depicted of a representative PEN/PET film (25/75 wt %) before and after uniaxial drawing, using two polarization geometries. Before drawing, there is no preferred orientation since the sample is essentially isotropic at a molecular level; thus, no differences are found between VV and HH scattering intensities for all spectral features. However, when the sample is stretched, e.g., up to a draw ratio $\lambda = 4$, the VV and HH spectra develop differences in relative band intensities. The extent of such differences depends on the position of the sample, *v* or *h*, with respect to the laboratory-fixed coordinates, and reflects the anisotropy induced by the drawing process. In both cases, the scattering intensities of the skeletal vibrational modes are higher in the parallel to the draw direction polarization geometries, *h*-HH or *v*-VV, than in the corresponding cross-polarization geometries, *h*-VV or *v*-HH. That means there are more scatterers of disubstituted benzene and naphthalene rings in the *h*-HH or *v*-VV geometries, more benzene and naphthalene rings aligned toward the draw direction, and more macromolecular chains parallel to the draw direction.

In Figure 7, coupled *h*-HH and *h*-VV polarized Raman spectra are shown of PEN, PET, and PEN/PET (25/75 wt %) copolymer films stretched up to 10−15 °C above

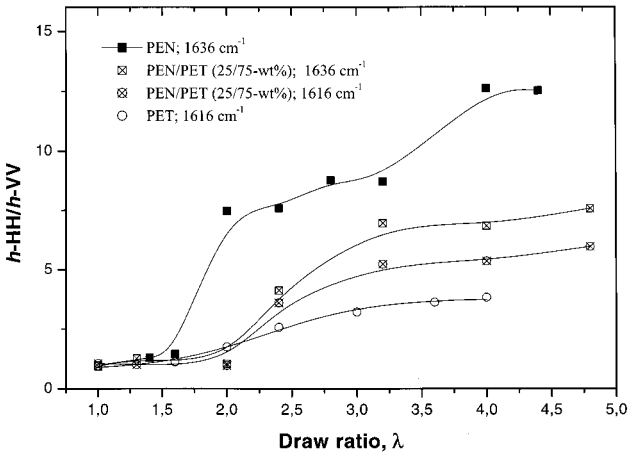

Figure 8. Polarization ratio, *h*-HH/*h*-VV, of PEN, PEN/PET (25/75 wt %) copolymer, and PET for the disubstituted phenyl (at 1616 cm^{-1}) and naphthalene (at 1636 cm^{-1}) ring symmetric stretch as a function of the draw ratio for uniaxial stretching films. Lines are drawn to guide the eye.

their glass transition temperatures at different draw ratios. Increasing the draw ratio, from $\lambda = 1$ to $\lambda \sim 4$, the intensities of the skeletal Raman bands of PEN are abruptly enhanced at around $\lambda = 2 \pm 0.5$ in the parallel to the draw axis polarization geometry, *h*-HH, relative to the corresponding of the cross-polarization geometry, *h*-VV. At the same draw ratio range neck formation occurred in the drawn film accounting for a highly localized cooperative orientation of flat naphthalene groups parallel to the surface of films in terms of an isotropic−nematic order transition manifesting macroscopically as a neck.[29] The addition of 75 wt % of PET to PEN produces a PEN/PET copolymer with a small average PEN sequence length (see ^{1}H NMR data in Table 2) that hinders the preferential orientation of the naphthalene planes parallel to one another and to the film surface, reducing thus both the longitudinal molecular orientation and the neck formation. This is also confirmed in Figure 8, where the behavior of the skeletal Raman bands of disubstituted benzene and naphthalene rings situated at 1616 (PET) and 1636 cm^{-1} (PEN) is presented in terms of the polarization ratio, *h*-HH/*h*-VV, vs draw ratio, λ, in both homopolymers and the copolymer. From these qualitative results it is clear that in the copolymer an increased orientation of PET segments and an attenuation of the neck formation of PEN occur.

Moreover, we may mention here that, apart from the 1636 cm^{-1} band used in this work, other Raman bands related also to naphthalene ring vibrational modes, like those situated at 1393 and 1482 cm^{-1}, might be additionally utilized for the evaluation of the orientation parameters of PEN segments. However, these bands are both less sensitive to the drawing process compared with that at 1636 cm^{-1}. In Figure 7, where *h*-HH and *h*-VV coupled polarized Raman spectra are depicted for both PEN and PEN/PET (25/75 wt %) samples, it is clearly seen that the Raman band at 1636 cm^{-1} presents a higher polarization ratio (*h*-HH/*h*-VV) than that at 1393 cm^{-1}, manifesting a higher sensitivity to the molecular orientation. The same conclusion, although to a lesser extent, holds when the 1636 cm^{-1} band is attentively compared with that at 1482 cm^{-1}; the latter besides that exhibits low scattering intensity.

Analysis of Raman Spectra. To deduce P_2 and P_4, we adopted the analysis of Pigeon et al.,[30] based on the theory of Bower[8] for the determination of the distribution of the molecular orientation using Raman spectra. Two sets of coordinates axes are fixed: one referred to the sample, $Ox_1x_2x_3$, and the second one to the experimental setup and the laboratory, $OX_1X_2X_3$. The total Raman scattering intensity is given by

$$I_s = I_0 \sum \left(\sum_{i,j} I_i I'_j a_{ij}\right)^2 \tag{3}$$

I_i and I'_j are the polarized direction of the incident and scattered light with respect to the set of axes fixed in the sample.

The experimental values are of the form $I_0 = \sum a_{ij}a_{pq}$, and in the case of uniaxial statistical symmetry with no preferred orientation one can write

$$\sum a_{ij}a_{pq} = 4\pi^2 N_0 \sum M_{l00} A_{l00}^{\ ijpq} \tag{4}$$

M_{l00} is expressed in terms of Legender polynomials: $M_{l00} = (1/4\pi^2)\{(2\lambda + 1)/2\}^{1/2}\langle P_l(\cos\theta)\rangle$ ($l = 0, 2, 4$), $A_{l00}^{\ ijpq}$ is a sum containing a_1, a_2, and a_3. There are only five independent nonzero sums $\sum a_{ij}a_{pq}$ that are of the form $\sum a_{ii}a_{jj}$ and $\sum a_{ij}^2$, in agreement with the analysis of Mead.[31] Citra has also shown[32] how the above five components of $a_{ij}a_{pq}$ are related to measurable quantities. The analytical expressions of the above nonzero sums as well as the procedure followed for the determination of the second and fourth term of the orientation distribution function from backscattering polarized Raman measurements under the hypothesis of a cylindrical Raman tensor have been given in detail elsewhere.[9−11] For PET segments, the assumption that the Raman tensor of the C_1-C_4 benzene ring vibration at 1616 cm^{-1} is cylindrical is justified by numerous studies of PET reported in the literature,[33] since they clearly show that a comparison of orientation moments with and without the assumption of uniaxial Raman tensor leads to the conclusion that the assumption is reasonable. For PEN segments, becuse of the lack of related studies concerning the Raman tensor for the C_2-C_6 naphthalene ring vibration at 1636 cm^{-1} and although there is no solid basis for its symmetry, we have arbitrarily assumed it as a cylindrical one and used it for only the comparison of PEN segments orientation in different copolymer type films. The results derived below (in Figures 9 and 10) are used to just denote trends of the molecular orientation; nevertheless, they are consistent with the corresponding variation of the polarization ratio with draw ratio, shown in Figure 8, which offers an indisputable means for the estimation of orientational parameters. Moreover, because of the moderate draw rate employed in the present study ($\dot{\epsilon}_{max} = 0.2\ s^{-1}$), we also assume that the elements of the considered Raman tensor do not vary with drawing,[3] and the calculation of the Raman tensors' ratios from corresponding isotropic samples is thus considered legitimate.

In this context, the analysis of the polarized Raman spectra obtained from quasi-amorphous polymer films for homopolymers and copolymers in the whole concentration range is summarized in Figure 9 as P_2 values of PET (on the top) and PEN (on the bottom) segments vs draw ratio, λ. The polymer films were drawn at

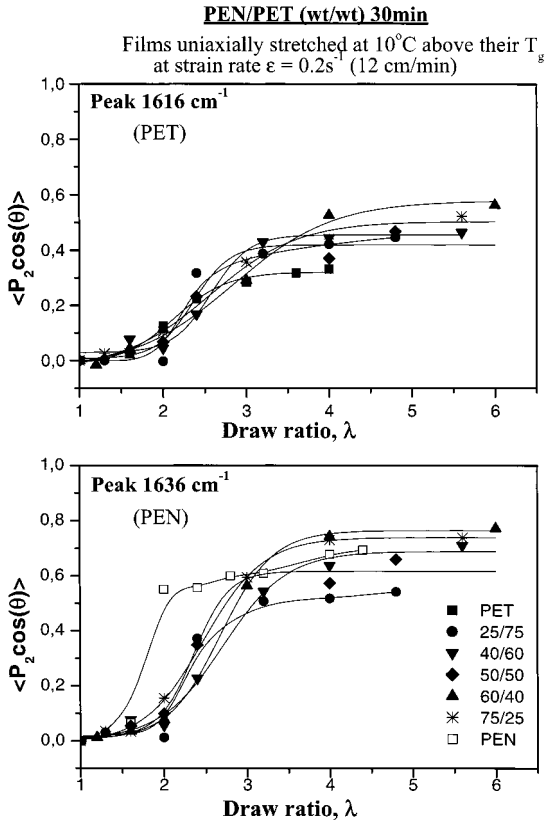

Figure 9. Second moment, P_2, of the orientation distribution function of PEN/PET (wt/wt) copolymers in different compositions for PET (on the top) and PEN segments (on the bottom) from Raman measurements as a function of the draw ratio. In both cases, the results of the corresponding homopolymers are also included for comparison. Lines are drawn to guide the eye.

approximately 10 °C above the corresponding T_g's and at a strain rate of $\dot{\epsilon} = 0.2\ s^{-1}$. The general picture of the variation of orientation, $\langle P_2(\cos\theta)\rangle$, with extension, at the above specified stretching parameters, is more or less the same for all polymer films. In the first regime the deformation increases rapidly with draw ratio; it then levels off and reaches an equilibrium plateau value.

In homopolymer PEN, the P_2 exhibits a rapid rise at $\lambda = 2$, after which it reaches almost a plateau at approximately 0.65. This rise in the P_2 coincides with the appearance of a neck. A further increase in deformation results in propagation and eventual disappearance of the neck. This phenomenon has also been observed with birefringence and microbeam wide-angle X-ray diffraction measurements[29] and has been attributed to a double orientation, orientation of the polymer chains along the draw direction, and orientation of the naphthalene planes parallel to the film surface. This behavior resembles an isotropic to nematic structural transition, which occurs at highly localized regions of the sample, thereby manifesting itself as a neck.

In PEN/PET copolymers, because of the nearly random sequences of monomer units and the presence of the stiffer PEN arrangements in the macromolecular chains, PET segments are oriented to a higher degree than in the homopolymer. More precisely, the P_2 plateau values of PET segments from 0.32 in the homopolymer are enhanced to 0.44 and 0.55 for PEN/PET copolymers bearing 25/75 and 60/40 wt % compositions, respectively.

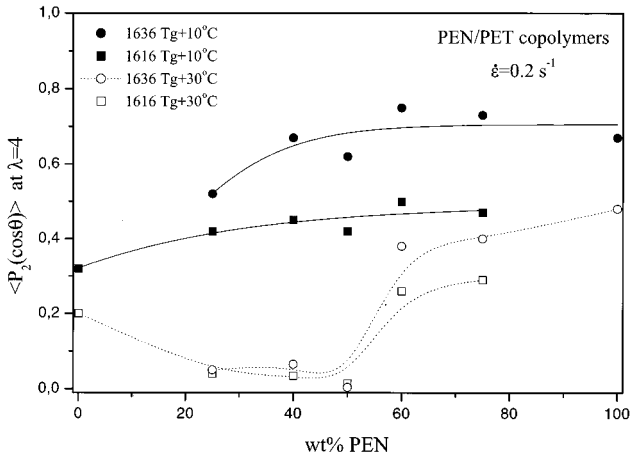

Figure 10. Second moment, P_2, of the orientation distribution function for PEN (●, ○) and PET (■, □) segments of PEN/PET (wt/wt) copolymer specimens, drawn at the same draw ration, $\lambda = 4$, at two stretching temperatures, $T_g + 10$ °C (solid lines) and $T_g + 30$ °C (dotted lines), from Raman measurements as a function of PEN (wt %) composition in the copolymers. Lines are drawn to guide the eye.

From the other hand, PEN segments exhibit a smoother increase in P_2, reaching comparable homopolymer PEN plateau values but at a higher draw ratio. A similar reduction of PEN necking behavior was observed[34] after addition of poly(ether imide) (PEI) in PEN in the form of deformed as-cast amorphous PEN/PEI blends.

It is also worth noticing that in polymer mixtures with naphthalate average segment length larger than the terephthalate one, as ^{1}H NMR measurements revealed (Table 2) for PEN/PET (60/40) composition, PEN segments demonstrate a maximum of 0.75 in the P_2 plateau values, being even higher than the corresponding values estimated for the homopolymer. PET sequences most probably act as kind of flexible spacer for the stiffer PEN segments, accounting for a higher extension ratio for both types of arrangements.

For PEN/PET copolymers, an overall picture of the development of the second moment, P_2, of the orientation distribution function with PEN weight precent is given in Figure 10. The values depicted here were obtained from the P_2 equilibrium plateau values, at $\lambda = 4$, for PEN/PET copolymers stretched at a strain rate of $\dot{\epsilon} = 0.2\ s^{-1}$ and at two different draw temperatures, 10 and 30 °C above the corresponding T_g's. For copolymer films drawn at $T_g + 10$ °C, the P_2 plateau values evolution of both PEN and PET segments indicate a similar segmental orientation distribution with some small discrepancies already invoked above. However, the PEN/PET copolymer specimens drawn at $T_g + 30$ °C exhibit different degrees of segmental relaxation that depend on the concentration range. For polymer mixtures with dominant PET number-average segment length, $L_{PET} > L_{PEN}$ (see Table 2), that is for samples with PEN mole fraction ≤50%, almost complete segmental relaxation for both PEN and PET segments occurs. On the other hand, copolymers with dominant PEN average segment length, $L_{PEN} > L_{PET}$, when drawn 30 °C above their T_g's demonstrate a moderate segmental orientation, although both PEN and PET segments remain at the same orientation level with corresponding homopolymers. The dynamic mechanical behavior of the PEN/PET samples reported in Figure 10 has been also investigated. These dynamic tensile modulus data,

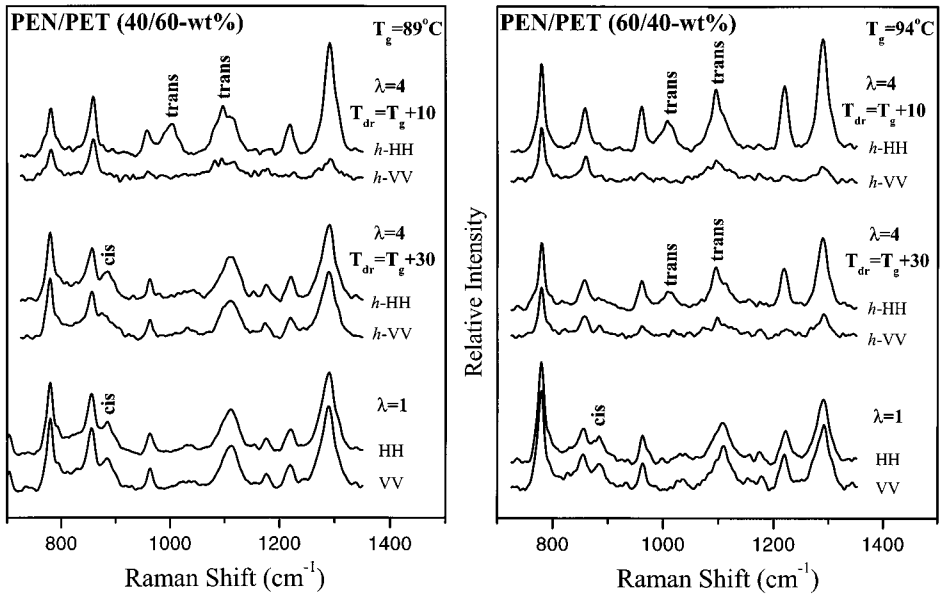

Figure 11. Polarized Raman spectra in the ethylene glycol fragment spectral range for PEN/PET (40/60 wt %) (on the left) and (60/40 wt %) (on the right) copolymer specimens before (bottom) and after drawing, to the same draw ratio, $\lambda = 4$, at two different draw temperatures, $T_g + 30$ °C (middle) and $T_g + 10$ °C (top).

Table 3. Dynamic Tensile Moduli (E') at 10 Hz and 25 °C

PEN/PET (wt/wt)	E' (GPa)		
	$\lambda = 1$	$\lambda = 4$, $T_g + 10$	$\lambda = 4$, $T_g + 30$
0/100	13.5	26.9	23.1
25/75	16.1	64.3	10.5
40/60	18.4	67.2	18.9
50/50	19.1	55.6	09.0
60/40	20.9	92.0	36.0
75/25	16.6	82.8	41.5
100/0	14.5	75.1	52.1

shown in Table 3, depict a similar polarized Raman spectra picture revealing relevant stretched induced orientation and relaxation behavior of the molecular segments in PEN/PET copolymers. It is anticipated that these PEN/PET copolymer specimens with their orientation relaxation discrepancies may constitute an interesting system for dielectric measurements, inasmuch as the molecular origin of a relaxation process is related to its morphological environment; the latter can be easily monitored in these mostly random copolymers and gives the opportunity to learn more about the reorientation dynamics during drawing.

Furthermore, in another attempt of the present study to get a more elaborate picture of these orientation relaxation discrepancies, the polarized FT-Raman spectra of two representative PEN/PET copolymer mixtures revealing different degrees of segmental relaxation, when drawn at different draw temperatures, are compared in the twinned Figure 11, in the ethylene glycol fragment spectral range. It is well-known that the Raman bands of glycol residue are conformation-sensitive.[35] In the crystalline state, PET is present in an almost planar form, and the corresponding Raman band, attributed to $O-CH_2$ stretching of the trans isomer, is situated at 998 cm^{-1}. Another Raman band at ~1095 cm^{-1} was mainly attributed to the contribution of the trans ethylene glycol C−C bonds. The Raman spectrum of an annealed PEN sample exhibits the related scattered peaks at ~1015 and 1095 cm^{-1}. In the amorphous state, PET and PEN have a more sophisticated conformational composition, and both trans and gauche conformations of the corresponding segments are present.

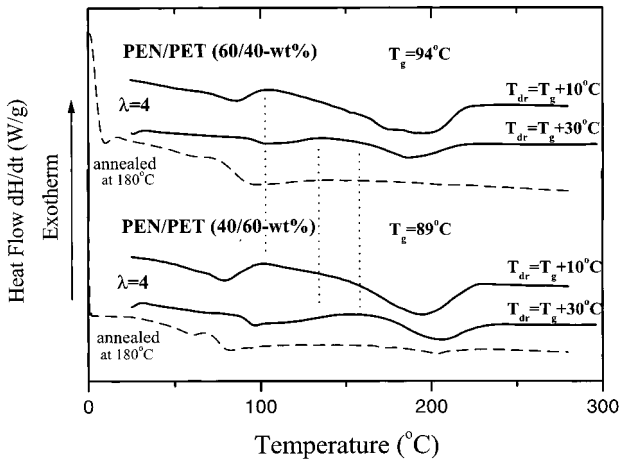

Figure 12. DSC scans first run curves of PEN/PET (60/40 wt %) (on the top) and (40/60 wt %) (on the bottom) copolymers drawn to $\lambda = 4$ at two different stretching temperatures, $T_g + 10$ °C and $T_g + 30$ °C. Thermograms of amorphous samples that have been annealed for 20 min at 180 °C are also depicted.

The Raman bands at ~885 cm^{-1} are assigned to a gauche conformation of the ethylene glycol segments in both homopolymers. It has been already invoked for PET that, in general, deformation induces a conformational transition from the "coiled" gauche chain to the "extended" trans.[36] The polarized Raman spectra shown in Figure 11 reveal a gauche−trans conformational change for the drawn PEN/PET samples only in the case they demonstrate differentiation in the Raman scattering intensities in the parallel and cross to the draw axis polarization geometries accounting for a certain degree of molecular orientation, in accordance with the results of Figure 9. For comparison, the polarized Raman spectra of the corresponding quasi-amorphous isotropic samples are given at the bottom of the twinned Figure 11.

In addition, the first run DSC scans from the above couples of drawn samples have been obtained, and they are depicted in Figure 12. For comparison, the first run DSC scans of the corresponding samples annealed for

20 min at 180 °C are also shown. For both PEN/PET samples drawn at $T_g + 10$ °C, the DSC scans show a broad exotherm at 100−140 °C which might be attributed[37] to the crystallization of oriented amorphous materials. For PEN/PET samples drawn at $T_g + 30$, no such significant contribution takes place although the crystallization of the sample that maintains a certain degree of molecular orientation (60/40) occurs at a lower temperature (∼135 °C) than that which relaxes (∼160 °C) because most probably the energy required for crystallization decreases as the chains become oriented. We have to note that although both PEN/PET (60/40 and 40/60 wt %) isotropic samples do not crystallize, the PEN/PET (40/60 wt %) sample drawn at $T_g + 30$ presents a certain degree of crystallization during the DSC scan although not oriented. This indicates that even though this drawn sample manifests complete segmental relaxation, most probably it maintains a certain anisotropy of chain disposition, and a mesophase link of the amorphous to the crystalline phase might be developed.

In PEN/PET random copolymers, for samples that have been rapidly quenched during drawing, transmission X-ray diffraction patterns revealed[38] strong evidence of a transient smectic phase, which appears to be the precursor of strain-induced crystallization. The presence of three-dimensional order in crystals based on non-liquid-crystalline systems of random copolymers has received considerable attention, and models applied to examine their behavior have been already built up from the schools of Windle[39] and Blackwell[40] and utilized with respect to the structure of liquid-crystalline random copolymer systems. Both models involve a degree of longitudinal register between the chains forming the crystal. Windle and co-workers proposed[39] the nonperiodic layer (NPL) crystallite model. They considered the possibility of longer longitudinal motions, which could enable sequence matching over limited distances in the chain direction to give nonperiodic layer (NPL) crystallites. Blackwell and co-workers proposed[40] the plane start model. They demonstrated that a single plane of longitudinal register imposed normal to the chains would produce a degree of three-dimensional order over a limited volume.

Nevertheless, independent crystallization mainly of the major component in PEN/PET polymer mixtures has already occurred from amorphous samples annealed above their cold crystallization temperatures.[41] The variation in the preparation techniques of similar samples might most probably account for differences in the origin of the crystallization process.[42] However, in the present study, because of the preparation procedure pursued, the cocrystallization seems the most probable process involved, although persistence of microcrystalline domains in PEN and PET which might behave as initiators of the orientation process, it is not easy to be either rejected or claimed for these PEN/PET mostly random polymer blends.

In PEN/PET copolymers drawn at $T_g + 10$ °C, the crystalline stacks induced by the drawing with the eventual support of the rigid amorphous phase (mesophase) most probably restrict the mobile amorphous layers in the cooperative length scale range, $\xi\alpha$, inhibiting cooperative segmental motions. Considering the larger extension of PEN monomer compared to PET,[43] a higher value of $\xi\alpha$ is expected for copolymers with $L_{PEN} > L_{PET}$, just as in the case of the PEN/PET (60/40 wt %) samples. According to the Adams and Gibbs theory,[44] $\xi\alpha$ decreases with increasing temperature. So, in the PEN/PET (40/60 wt %) copolymer drawn at $T_g + 30$ °C, $\xi\alpha$ was most probably decreased to the point that shorter length scale segmental motions have been activated.

In this context, it is necessary to make a note of other important parameters that might influence the molecular orientation of PEN/PET copolymers, such as the time the draw procedure is accomplished, which depends mainly on the draw rate used, and the extent of the draw ratio attained.

Conclusions

A series of random copolymers of PEN and PET were synthesized and characterized by DSC, ^{1}H NMR measurements, and FT-Raman spectroscopy. Polarized Raman measurements, obtained via a flexible custom-made micro-Raman instrumentation, have been employed to evaluate the molecular orientation of PEN and PET segments of quasi-amorphous PEN/PET copolymer samples. These Raman orientation data have revealed that in the copolymers PET segments are oriented to a higher degree than in the homopolymer, while the neck formation of PEN lies down under the incorporation of PET. Moreover, in the PEN/PET polymer mixtures with a PEN average segment length higher than that of PET, the naphthalate monomer sequences exhibit even higher homopolymer molecular orientation. In addition, PEN/PET films stretched at temperatures 30 °C higher than the corresponding T_g's demonstrate significant relaxation discrepancies that are accompanied by conformational changes of the ethylene moieties and are supported by tensile modulus data as well. A note is made of the fact that the molecular orientation of PEN/PET copolymers is very sensitive to the draw temperature, revealing the importance of the length and the degree of alternation for PEN and PET sequences.

Acknowledgment. The authors are indebted to Mr. D. Vachliotis (Center of Instrumental Analysis of University of Patras) for performing the ^{1}H NMR measurements and to Prof. J. Kallitsis (Laboratory of Polymer Science, Department of Chemistry, University of Patras) for giving the opportunity to perform dynamic mechanical analysis measurements.

References and Notes

(1) Ward, I. M. *Structure and Properties of Oriented Polymers*; Chapman & Hall: London, 1997.
(2) Bruggeman, A.; Buijs, J. A. H. M. *Polymer* **1996**, *37*, 5639.
(3) Lesko, C. C. C.; Rabolt, J. F.; Ikeda, R. M.; Chase, B.; Kennedy, A. *J. Mol. Struct.* **2000**, *521*, 127.
(4) Yoshiyuki, N.; Hidematsu, S.; Kazuyuki, S. *Polymer* **1994**, *35*, 1452.
(5) Buffeteau, T.; Desbat, B.; Bokobza, L. *Polymer* **1995**, *36*, 4339.
(6) Pellerin, C.; Prud'homme, R. E.; Pezolet, M. *Macromolecules* **2000**, *33*, 7009.
(7) Roe, R.-J *J. Appl. Phys.* **1965**, *36*, 2024. Roe, R.-J. *J. Polym. Sci., Part A-2* **1970**, *8*, 1187.
(8) Bower, D. I. *J. Polym. Sci., Polym. Phys. Ed.* **1972**, *10*, 2135.
(9) (a) Voyiatzis, G.; Petekidis, G.; Vlassopoulos, D.; Kamitsos, E. I.; Bruggeman, A. *Macromolecules* **1996**, *29*, 2244. (b) Andrikopoulos, K.; Vlassopoulos, D.; Voyiatzis, G. A.; Yiannopoulos, Y. D.; Kamitsos, E. I. *Macromolecules* **1998**, *31*, 5465.
(10) Deimede, V.; Andrikopoulos, K. S.; Voyiatzis, G. A.; Kostandakopoulou, F.; Kallitsis, J. K. *Macromolecules* **1999**, *32*, 8848.

(11) Voyiatzis, G. A.; Andrikopoulos, K. S.; Papatheodorou, G. N.; Kamitsos, E. I.; Chryssikos, G. D.; Kapoutsis, J. A.; Anastasiadis, S. H.; Fytas, G. *Macromolecules* **2000**, *33*, 5613.
(12) Schlotter, N. E. In *Encyclopedia of Polymer Science and Engineering*, 2nd ed.; Mark, H. F., Bikales, N., Ovenberger, C. G., Megnes, G., Eds.; Wiley: New York, 1988.
(13) Tullo, A. *CENEAR* **2000**, *78* (21), 25.
(14) Abtal, E.; Prud'homme, R. E. *Polymer* **1996**, *37*, 3805.
(15) McGonigle, E.-A.; Liggat, J. J.; Pethrick, R. A.; Jenkins, S. D.; Daly, J. H.; Hayward, D. *Polymer* **2001**, *42*, 2413.
(16) Wang Y. D.; Cakmak, M. *Polymer* **2001**, *42*, 4233.
(17) Rinderknecht, S.; Brisson, J. *Macromolecules* **1999**, *32*, 8509.
(18) Chung, H.; Lee, C.; Han, H. *Polymer* **2001**, *42*, 319.
(19) Lee, S. C.; Yoon, K. H.; Park, I. H.; Kim, H. C.; Son, T. W. *Polymer* **1997**, *38*, 4831.
(20) Wendling, J.; Gusev, A.; Suter, U. W. *Macromolecules* **1998**, *31*, 2509.
(21) Aoki, Y.; Li, L.; Amari, T.; Nishimura, K.; Arashiro, Y. *Macromolecules* **1999**, *32*, 1923.
(22) McDowell, C. C.; Freeman, B. D.; McNeely, G. W. *J. Polym. Sci., Part B: Polym. Phys.* **1999**, *37*, 2973.
(23) Collins, S.; Kenwright, A. M.; Pawson, C.; Peace, S. K.; Richards, R. W.; MacDonald, W. A.; Mills, P. *Macromolecules* **2000**, *33*, 2974.
(24) Becker, O.; Simon, G. P.; Rieckmann, T.; Forsythe, J.; Rosu, R.; Völker, S.; O'Shea, M. *Polymer* **2001**, *42*, 1921.
(25) Merino, J. C.; Pastor, J. M.; De Saga, J. A. *Polymer* **1985**, *26*, 383.
(26) Rueda, D. R.; Varkalis, A. *J. Polym. Sci., Polym. Phys. Ed.* **1995**, *33*, 2263.
(27) Stewart, M. E.; Cox, A. J.; Naylor, D. M. *Polymer* **1993**, *34*, 4060.
(28) Yamadera, R.; Murano, M. *J. Polym. Sci., Part A* **1967**, *5*, 2259.
(29) Cakmak, M.; Lee, S. W. *Polymer* **1995**, *36*, 4039.
(30) Pigeon, M.; Prud'homme, R. E.; Pezolet, M. *Macromolecules* **1991**, *24*, 5687.
(31) Mead, D. W. Personal communication, 1996.
(32) Citra, M. J.; Chase, B.; Ikeda, R. M.; Gardner, K. H. *Macromolecules* **1995**, *28*, 4007.
(33) (a) Everall, N. J. *Appl. Spectrosc.* **1998**, *52*, 1498. (b) Lapersonne, P.; Bower, D. I.; Ward, I. M. *Polymer* **1992**, *33*, 1266. (c) Purvis, J.; Bower, D. I. *J. Polym. Sci., Polym. Phys. Ed.* **1976**, *14*, 1461. (d) Purvis, J.; Bower, D. I.; Ward, I. M. *Polymer* **1973**, *14*, 398.
(34) Cakmak, M.; Kim, J. C. *J. Appl. Polym. Sci.* **1997**, *65*, 2059.
(35) Taylor, D. J. R.; Stepto, R. F. T.; Bleackley, M.; Ward, I. M. *Phys. Chem. Chem. Phys.* **1999**, *1*, 2065.
(36) Rodriguez-Cabello, J. C.; Merino, J. C.; Quintanilla, L.; Pastor, J. M. *J. Appl. Polym. Sci.* **1996**, *62*, 1953.
(37) Mattwes, R. G.; Ajji, A.; Dumoulin, M. M.; Prud'homme, R. E. *Polymer* **2000**, *41*, 7139.
(38) Welsh, G. E.; Blundell, D. J.; Windle, A. H. *Macromolecules* **1998**, *31*, 7562.
(39) (a) Hanna, S.; Windle, A. H. *Polymer* **1988**, *29*, 207. (b) Hanna, S.; Romo-Uribe, A.; Windle, A. H. *Nature (London)* **1993**, *366*, 546.
(40) (a) Gutierrez, G. A.; Chivers, R. A.; Blackwell, J.; Stamatoff, J. B.; Yoon, H. *Polymer* **1983**, *24*, 937. (b) Biswas, A.; Blackwell, J. *Macromolecules* **1988**, *21*, 3158.
(41) Wu, G.; Cuculo, J. A. *Polymer* **1999**, *40*, 1011.
(42) Patcheak, T. D.; Jabarin, S. A. *Polymer* **2001**, *42*, 8975 and references therein.
(43) Nogales, A.; Denchev, Z.; Sics, I.; Ezquerra, T. A. *Macromolecules* **2000**, *33*, 9367.
(44) Adams, G.; Gibbs, J. H. *J. Chem. Phys.* **1965**, *43*, 139.

MA011229H